

# Direct evidence of the receding ‘torus’ around central nuclei of powerful radio sources

T. G. Arshakian<sup>1,2</sup>

<sup>1</sup> Max-Planck-Institut für Radioastronomie (MPIfR), Auf dem Hügel 69, 53121 Bonn, Germany  
e-mail: tigar@mpifr-bonn.mpg.de

<sup>2</sup> Byurakan Astrophysical Observatory, Aragatsotn prov. 378433, Armenia and Isaac Newton Institute of Chile, Armenian Branch

17 September 2004

**Abstract.** The presence of obscuring material (or a dusty ‘torus’) in active galactic nuclei (AGN) is central to the unification model for AGN. Two models, the multi-population model for radio sources and the receding torus model, are capable of describing observational properties of powerful radio galaxies and radio quasars. Here, I study the changes of the opening angle of the obscuring torus with radio luminosity at 151 MHz, [O III] emission-line luminosity and cosmic epoch aiming to discriminate between two working models. An analytical expression relating the half opening angle of the torus to the mean projected linear sizes of double radio galaxies and quasars is derived. The sizes of powerful double radio sources taken from the combined sample of 3CRR, 6CE and 7CR complete samples are used to estimate the torus opening angle. I found a statistically significant correlation between the half opening angle of the torus and [O III] emission-line luminosity. The opening angle increases from 20° to 60° with increasing [O III] emission-line luminosity. This correlation is interpreted as direct evidence of the receding torus around central engines of powerful double radio sources.

**Key words.** Galaxies: active – Radio continuum: galaxies – Methods: analytical

## 1. Introduction

Spectropolarimetric observations of Seyfert 2 galaxies (Antonucci & Miller 1985; Miller & Goodrich 1990) suggested an orientation-based unification scheme for active galactic nuclei (AGN). An optically thick molecular torus obscuring the AGN permits a unification of Seyfert 1 and Seyfert 2 galaxies by proposing that they are intrinsically the same objects viewed at different angles to the axis of the torus. This model was invoked by Scheuer (1987) and Barthel (1989) to account for the orientation-dependent appearance of powerful radio sources, which can appear as radio galaxies or quasars. According to the standard picture, the torus hides the AGN and broad-line region of a radio galaxy, whereas for quasars these are viewed directly for a quasar down the ionization cone. The opening angle of the torus defines the cone angle and the half opening angle is the critical angle ( $\theta_c \sim 45^\circ$ ; Barthel 1989) at which the transition between radio galaxies and quasars occurs. The narrow-line regions have extended kpc-scale structure and therefore are visible for any orientation of the torus. There is considerable multi-band observational evidence supporting the unification scheme for radio galaxies and quasars. This comes from the X-ray detection of inverse Compton scattered photons (Brunetti et al. 1997) and polarized (scattered) emission lines from hidden quasars in some radio galaxies (Antonucci & Miller 1985),

from the direct detection of unabsorbed soft and hard X-ray emissions from quasars (e.g. 3C 109, Allen and Fabian 1992; Cyg A, Ueno et al. 1994; 3C 295, Brunetti et al. 2001; 3C 265, Bondi et al. 2004), from the detection of comparable far-infrared emission from the high-redshift ( $z > 0.8$ ) radio galaxies and quasars (e.g. Meisenheimer et al. 2001; Haas et al. 2004), from the difference of the mid-infrared spectral energy distribution in the broad-line and narrow-line AGN (Siebenmorgen et al. 2004), from the detection of superluminal radio knots on parsec-scales (Vermuelen & Cohen 1994), and from the presence of supermassive black holes and relativistic jets in both radio galaxies and quasars (McLure & Dunlop 2002; Laing 1988; Garrington et al. 1988).

A single opening angle can not account for two pieces of observational evidence: (i) at a given radio power the [O III] lines are weaker in radio galaxies than in quasars (Lawrence 1991; Simpson 2003), and (ii) the increase of the quasar fraction with increasing radio luminosity (Hill et al. 1996; Willott et al. 2000; Grimes et al. 2004). Lawrence (1991) suggested the receding torus model in which the dust evaporation radius of the torus depends on the luminosity of the photoionizing radiation of the AGN, which is assumed to be independent of the height of the torus. In this scenario the opening angle of the torus increases with increasing luminosity of the ionizing radiation,  $L_{\text{phot}}$ , from the AGN. This model accounts for the fact

that quasars are brighter in  $L_{\text{phot}}$  than radio galaxies (Lawrence 1991; Simpson 2003) in samples selected at low radio frequencies, and that the fraction of quasars increases with radio luminosity. Gopal-Krishna et al. (1996) showed that a wider opening angle with increasing radio luminosity could explain the problem of unification posed by the difference between the radio luminosity-size correlations for radio galaxies and quasars. In addition, Willott et al. (2000) found that the fraction of quasars decreases at low luminosities. They argued that this can be explained either by the receding torus model (decrease of  $\theta_c$  with decreasing radio luminosity), or by the existence of a second population of low-luminosity radio galaxies. Grimes et al. (2004) used a combined complete sample at 151 MHz to show that, in the luminosity-dependent unified scheme, a two-population model may explain the increase of the quasar fraction with  $L_{\text{phot}}$  as well as the emission-line differences between radio galaxies and quasars. They conclude that the effect of the receding torus may be important but it is not clear yet whether the receding torus is present in both populations.

The opening angle of the torus,  $\theta_c$ , defines the geometry of the torus (the inner radius and height) and appears to be an important parameter for understanding the evolutionary behaviour of the obscuring material and testing the torus model. In the Appendix, I derive an equation that allows the mean half opening angle of the torus  $\bar{\theta}_c$  to be estimated by means of the projected linear sizes of radio galaxies and quasars. In section 2 the equations for estimating  $\bar{\theta}_c$  are presented. The combined complete sample of radio sources is described in section 3. In section 4, the relations between the critical angle with the 151 MHz radio luminosity  $L_{151}$ , [O III] 5007-Å emission-line luminosity  $L_{[\text{O III}]}$  and cosmic epoch are investigated. In section 5, the receding torus model is discussed.

Throughout the paper a flat cosmology ( $\Omega_m + \Omega_\Lambda = 1$ ) with non-zero lambda,  $\Omega_m = 0.3$  and  $H_0 = 70 \text{ km s}^{-1} \text{ Mpc}^{-1}$  is used.

## 2. Equations for the opening angle of the torus

Powerful FR II (Fanaroff & Riley 1974) radio galaxies and quasars are associated with bipolar relativistic radio jets emerging from the AGN which form extended radio lobes on both sides of the AGN. The radio jets are almost aligned with the axes of the tori in FR II (Cyg A; Canalizo et al. 2004) and FRI radio sources (3C270, Jaffe et al. 1993; Verdoes Kleijn et al. 2001). The half opening angle of the torus is defined by the angle between the radio axis and the direction at which the division between radio galaxies and quasars occurs. Then the half opening angle of the torus can be estimated by means of the projected linear sizes of FR II radio galaxies and quasars; linear sizes of quasars appear to be systematically smaller than the linear sizes of radio galaxies (Barthel 1989) as a result of projection effects. In the Appendix, I derive an equation (7) for estimating the mean critical angle  $\bar{\theta}_{cs}$  from the ratio of the mean projected linear sizes of quasars  $\bar{l}_Q$  and the whole sample  $\bar{l}$ . The problem is solved for the sample of FR II radio sources having an isotropic distribution of radio axes over the sky. Low-frequency radio samples of radio sources are thought to be free from orientation biases and can be used in this analysis.

**Table 1.** The Kolmogorov-Smirnov test is used to estimate the significance level of the hypothesis that the [O III] emission-line luminosity (and radio luminosity) distributions of HEGs and quasars (QSOs), HEGs and WQs, and, QSOs and WQs are drawn from the same parent distribution.

$L_{[\text{O III}]}$ distribution	K-S test (%)	$L_{151}$ distribution	K-S test (%)
QSO-HEG	99.99	QSO-HEG	99.66
QSO-WQ	98.77	QSO-WQ	99.81
HEG-WQ	16.60	HEG-WQ	79.47

Another independent way to estimate the half opening angle is to consider the number of quasars  $N_Q$  and the number of radio galaxies and quasars  $N_{G+Q}$  in the low-frequency radio samples,

$$\bar{\theta}_{cf} = \arccos\left(1 - \frac{N_Q}{N_{G+Q}}\right). \quad (1)$$

If the unified schemes for FR II radio galaxies and quasars is valid then one should expect a correlation between  $\bar{\theta}_{cf}$  and  $\bar{\theta}_{cs}$ , which are independent estimates.

## 3. The sample and selection criteria

I use a combined sample of three complete low-frequency samples (Grimes et al. 2004)<sup>1</sup>, made up of the 3CRR, 6CE and 7CRS samples (Laing, Riley & Longair 1983; Rawlings, Eales & Lacy 2001; Willott et al. 2002). This contains 302 radio sources all having extended radio structure on kiloparsec-scales. I then excluded 3C48, 3C287 and 3C343 because they are complex with no clear double lobe structure (Laing et al. 1983). Three other sources were excluded: 3C231 because its radio emission is due to a starburst, 3C345 and 3C454.3 because their inclusion in the 3CRR sample is a result of Doppler boosting of the jet.

I adopted the classification of radio sources used by Grimes et al. (2004): high- and low-excitation narrow-line radio galaxies (HEGs and LEGs), weak quasars (WQs) and broad-line radio quasars. The category of weak quasars includes HEGs which are objects with weakly or heavily obscured broad-line nuclei seen indirectly (e.g., in broad wings of H $\alpha$  and Paschen lines, in optically-polarized light) and unobscured objects with weak broad-line optical nuclei.

There are 39 low-excitation radio galaxies in the sample which are believed to be a separate population independent from the high-excitation radio galaxies and radio quasars (Laing et al. 1994). Exclusion of these sources and FRI radio sources leaves a sample consisting of 237 FR II radio sources. The projected linear sizes (the apparent distance between radio lobes) of 3CRR sources are adopted from the 3CRR database<sup>2</sup>,

<sup>1</sup> The electronic version of the combined sample is available at <http://www-astro.physics.ox.ac.uk/~sr/grimes.html>.

<sup>2</sup> The electronic version of the 3CRR database can be found at <http://www.3crr.dyndns.org/cgi/database>

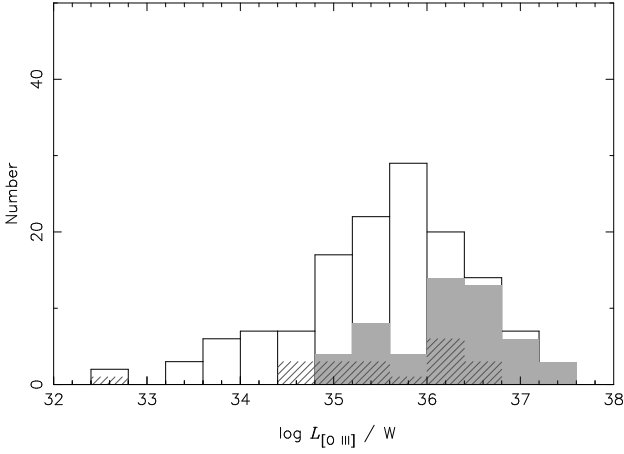


**Fig. 1.** The distribution of [O III] emission-line luminosity for 134 high-excitation narrow-line galaxies (open area), 52 quasars (grey area) and 20 weak quasars (hatched area) in the combined 3CRR, 6CE and 7CRS samples.

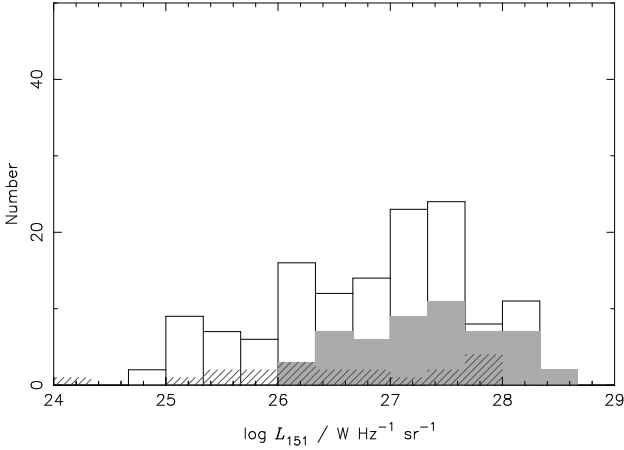


**Fig. 2.** The distribution of radio luminosity at 151 MHz for 134 HEGs (open area), 52 quasars (grey area) and 20 WQs (hatched area) in the combined sample.

and the sizes of 6CE and 7CRS sources are taken from the electronic version of the combined database<sup>1</sup>. The projected linear sizes vary over (1 to 2000) kpc over the range ( $1.6 \times 10^{24}$  to  $4.6 \times 10^{28}$ )  $\text{W Hz}^{-1} \text{sr}^{-1}$  of the 151 MHz radio luminosity.

The structure of FR II radio sources is influenced by environmental asymmetry, which becomes more important on small scales (Arshakian & Longair 2000). I excluded the compact steep-spectrum radio sources with typical sizes  $< 20$  kpc to avoid contamination of projection effects by interaction effects between a radio jet and interstellar medium (Barthel 1989). Their inclusion or exclusion does not introduce perceptible change in the results described below. The final sample consists of 206 FR II radio sources: 134 HEGs, 20 weak quasars and 52 quasars.

#### 4. Relations for the torus opening angle

The distribution of [O III] emission-line luminosities and radio luminosities of 206 FR II radio sources is shown in Figs. 1

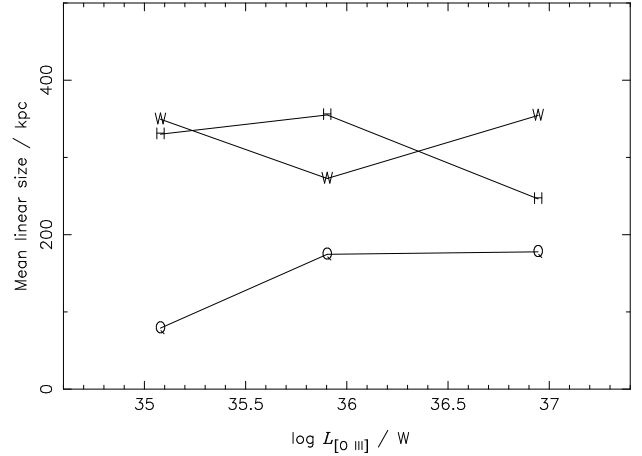


**Fig. 3.** Mean projected linear sizes of 206 FR II radio sources are calculated for three equal subsamples binned by [O III] emission-line luminosity. Quasars, weak quasars and HEGs are denoted by 'Q', 'W' and 'H' respectively.

and 2. There are 10 radio galaxies and two WQs with power  $< 2 \times 10^{25} \text{ W Hz}^{-1} \text{sr}^{-1}$ , typical for the transition region for FRI and FR II sources. Quasars appear to be more luminous than HEGs and WQs in both [O III] emission-lines and radio. The Kolmogorov-Smirnov test (Table 1) shows that the luminosity distributions ( $L_{[\text{O III}]}$  and  $L_{151}$ ) of quasars are different from the distributions of HEGs and WQs at high confidence level (mainly because of the lack of weak quasars in the sample), whilst the  $L_{[\text{O III}]}$  and  $L_{151}$  distributions of HEGs and WQs appear to be drawn from the same population. The later result is supported by the linear-size statistics of FR II sources: the mean projected linear size of weak quasars,  $(330 \pm 50)$  kpc, is comparable with the mean linear size of narrow-line HEGs,  $(320 \pm 30)$  kpc, and is twice as large as the mean size of quasars  $(162 \pm 19)$  kpc. This relation holds over the entire [O III] emission-line luminosity range (Fig. 3). The values of mean linear sizes of weak quasars are larger than those of quasars in three equal subsamples divided by [O III] emission-line luminosity. The same result is obtained when the sample is binned by 151 MHz radio luminosity. This supports the idea that HEGs and weak quasars are the same objects, where the later ones appear to have broad emission lines as a result of scattered light from the nucleus. Therefore in this analysis, the weak quasars are grouped with the HEGs rather than quasars. On the other hand, some of the WQs appear to be transitional objects (between quasars and HEGs) which are oriented near to the critical angle where the broad-line region is reddened but not totally obscured (Laing et al. 1994; Simpson et al. 1999) and hence they can be grouped with quasars. Therefore it is important to see how an exclusion of 20 WQs influences the final results and this will be discussed later in this section.

For the whole sample, I calculate the number of all radio sources  $N_{G+Q} = 206$  and quasars  $N_Q = 52$ , and their mean linear sizes  $\bar{l} = (279 \pm 21)$  kpc and  $\bar{l}_Q = (162 \pm 19)$  kpc respectively. Then the critical viewing angles,  $\theta_{cs} = 42^\circ \pm 7^\circ$  and  $\theta_{cf} = 42^\circ \pm 12^\circ$ , are estimated using equations (7) and (1). Two independent equations give similar results with the error being

**Table 2.** Estimates of critical angles,  $\theta_{cs}$  and  $\theta_{cf}$  and their errors in equal subsamples binned by  $L_{[\text{O III}]}$ . The first line of the table refers to the two sets of binned data, and the second line shows results of three sets of binned data.

(1)	(2)	(3)	(4)	(5)	(6)	(7)	(8)	(9)	(10)	(11)
$N_{\text{bin}}$	$\log(L_{[\text{O III}]} / W)$ bin width	$\log(\bar{L}_{[\text{O III}]} / W)$	$N_{\text{G+Q}}$	$N_{\text{Q}}$	$\theta_{cf} \pm \sigma_{\theta_{cf}}$ ( $^{\circ}$ )	<i>Fisher</i> test (%)	$\bar{l} \pm \sigma_{\bar{l}}$ (kpc)	$\bar{l}_{\text{Q}} \pm \sigma_{\bar{l}_{\text{Q}}}$ (kpc)	$\theta_{cs} \pm \sigma_{\theta_{cs}}$ ( $^{\circ}$ )	<i>Fisher</i> test (%)
2	32.43 – 35.81	35.51	103	12	$28 \pm 35$	48.6	$341 \pm 36$	$111 \pm 25$	$22 \pm 6$	99.4
	35.81 – 37.37	37.08	103	40	$52 \pm 12$		$217 \pm 19$	$177 \pm 22$	$63 \pm 14$	
3	32.43 – 35.38	35.08	68	6	$24 \pm 57$	17.5	$311 \pm 11$	$79 \pm 19$	$17 \pm 5$	97.4
	35.38 – 36.13	35.90	68	15	$39 \pm 24$		$308 \pm 43$	$175 \pm 39$	$41 \pm 12$	
	36.13 – 37.37	37.09	70	31	$56 \pm 13$		$225 \pm 23$	$178 \pm 25$	$59 \pm 14$	

Columns: (1) - The number of bins; (2) - [O III] luminosity bin width; (3) - Logarithm of the central value of the  $L_{[\text{O III}]}$  in the bin; (4,5) - Number of radio galaxies and quasars in the  $\log L_{[\text{O III}]}$  bin; (6) - The half opening angle of the torus estimated by fraction of quasars (eq. 1), and its standard error  $\sigma_{\theta_{cf}}$  is calculated assuming that  $\sigma_{N_{\text{G+Q}}} = \sqrt{N_{\text{G+Q}}}$  and  $\sigma_{N_{\text{Q}}} = \sqrt{N_{\text{Q}}}$ ; (7) - The confidence level of rejecting the null hypothesis that half opening angles  $\theta_{cf}$  of the torus estimated in different  $L_{[\text{O III}]}$  bins are equal. The variance analysis (the *Fisher* test) is used with two degrees of freedom,  $N_{\text{bin}} - 1$  and  $N_{\text{bin}}(N_{\text{G+Q}} - 1)$ ; (8,9) - The mean linear sizes of all sources (radio galaxies and quasars) and quasars, and their standard errors; (10) - The half opening angle of the torus and its standard error from eqs. (7) and (8); (11) - The confidence level for rejecting the null hypothesis that half opening angles  $\theta_{cs}$  of the torus are equal in different  $L_{[\text{O III}]}$  bins.

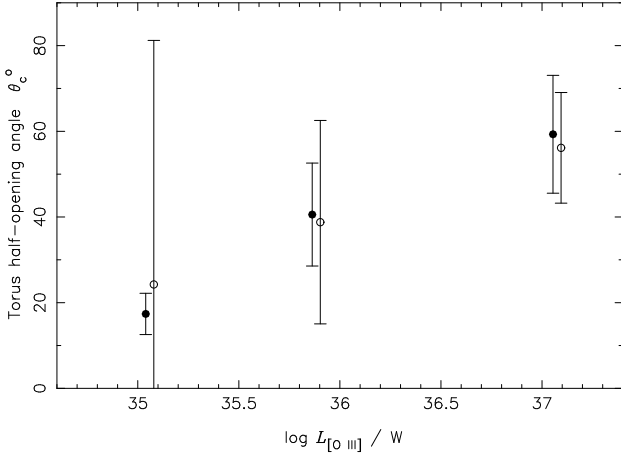


**Fig. 4.** The torus half opening angle calculated in three equal subsamples binned by [O III] emission-line luminosity (see Table 2). Critical angles  $\theta_{cs}$  estimated by the mean linear sizes of radio galaxies and quasars (eq. 7) are marked by filled circles, and open circles denote the critical angles  $\theta_{cf}$  calculated by the fraction of quasars (eq. 1). A *Fisher* test rejects the null hypothesis that  $\theta_{cs}$  are equal at 97.4 % confidence level. The filled circles are offset horizontally for illustrative purposes.  $1\sigma$  error bars are presented.

smaller for the mean linear size statistics (see Appendix for explanation). The true value of  $\bar{\theta}_{cs}$  lies between  $\sim 20^{\circ}$  and  $\sim 60^{\circ}$  at  $3\sigma$  (99.7 %) confidence level. There is a spread in the values of the critical viewing angle, which indicates that the simple unification scheme with constant  $\theta_c$  is not likely - there is some distribution of  $\theta_c$ . It would be interesting to see if the spread in  $\theta_c$  correlates with any other physical property of radio sources.

To examine the  $\bar{\theta}_c - L_{[\text{O III}]}$  dependence, I divided the sample into two equal subsamples (118 and 119 sources) by  $\log(L_{[\text{O III}]} / W) = 35.83$  and calculated  $\bar{\theta}_{cs}$  and  $\bar{\theta}_{cf}$  for each subsample (Table 2). Both,  $\bar{\theta}_{cs}$  and  $\bar{\theta}_{cf}$ , increase by a factor of two

**Table 3.** The significance (*Fisher* test) of the null hypothesis that the  $\theta_{cs}$  are equal in two equal subsamples divided by  $L_{[\text{O III}]}$ ,  $L_{151}$  and redshift  $z$ , respectively. Probabilities are calculated for: (1) the sample which includes 20 WQs grouped with HEGs rather than quasars, (2) the sample consisting only of HEGs and quasars, and (3) the sample which excludes 12 transitional sources with  $\log(L_{151} / W \text{ Hz}^{-1} \text{ sr}^{-1}) < 25.3$ .

Relation plane	<i>Fisher</i> test (%) (1)	<i>Fisher</i> test (%) (2)	<i>Fisher</i> test (%) (3)
$\bar{\theta}_{cs} - L_{[\text{O III}]}$	99.4	99.3	98.6
$\bar{\theta}_{cs} - L_{151}$	63.6	71.7	60.2
$\bar{\theta}_{cs} - z$	4.8	32.5	38.7

times from low to high  $L_{[\text{O III}]}$ . The *Fisher* test is used to test the null hypothesis that the mean critical angles are equal at low and high  $L_{[\text{O III}]}$ . For  $\theta_{cs}$  the null hypothesis is rejected at high confidence level (99 %), though it can not be rejected for  $\theta_{cf}$  (49 %) mainly because of the large errors involved (see Appendix). I also studied the  $\bar{\theta}_c - L_{[\text{O III}]}$  plane for three equal subsamples (Table 2; Fig. 4). The mean half opening angle increases from  $\sim 20^{\circ}$  to  $\sim 40^{\circ}$  and to  $\sim 60^{\circ}$  in three subsamples binned by [O III] emission-line luminosity, and the difference between the angles is still very significant (97 %). The difference becomes less significant ( $< 85\%$ ) when the sample is divided on four or more subsamples. The division into subsamples smaller than  $\sim 50$  objects does not allow a statistically significant correlation between  $\bar{\theta}_c$  and  $L_{[\text{O III}]}$  to be investigated. Also, the small samples may introduce fluctuations of  $\bar{\theta}_c$  due to statistical fluctuations in the orientation of radio sources (Saikia & Kulkarni 1994).

I repeated the analysis for the  $\bar{\theta}_c - L_{151}$  and  $\bar{\theta}_c - z$  relations. Both  $\bar{\theta}_{cs}$  and  $\bar{\theta}_{cf}$  estimated for two equal subsamples binned by

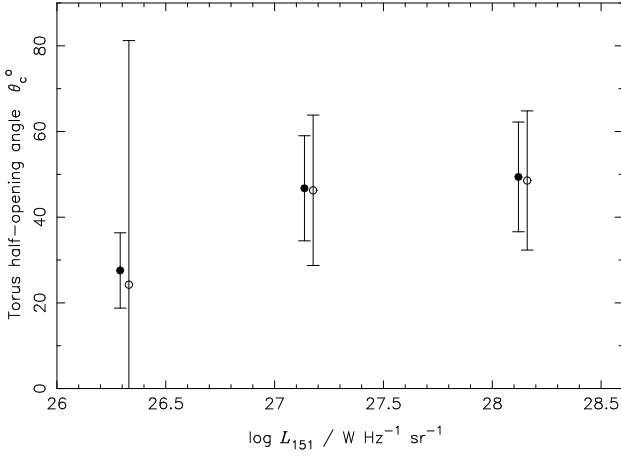


**Fig. 5.** The half opening angle of the torus calculated in three equal subsamples binned by radio luminosity. Designations are the same as in Fig. 4. The null hypothesis of equal critical angles  $\theta_{cs}$  (filled circles) can not be rejected (66%).

$L_{151}$  increase from low- to high-luminosities. This result was expected because the relation  $L_{[O III]} \propto L_{151}^{1.04}$  holds for the combined 3CRR, 6CE and 7CRS samples (Grimes et al. 2004). A Fisher test shows that the increase of  $\theta_{cs}$  with  $L_{151}$  is not statistically significant (Table 3; Fig. 5). No significant evolution of  $\bar{\theta}_{cs}$  or  $\bar{\theta}_{cf}$  is found with cosmic epoch  $z$ .

The results of this section stand even after excluding the WQs from the sample (Table 3). This indicates that the positive correlation in the  $\bar{\theta}_{cs} - L_{[O III]}$  plane is mainly due to HEGs and quasars. The significance of the correlation is still high after exclusion of transitional sources from the sample of 206 radio sources.

Let us consider the selection effects which might cause the positive correlation  $\bar{\theta}_c - L_{[O III]}$  seen in Fig. 4. Although there are problems with identifying the broad-line radio galaxies as low-luminosity quasars, Hardcastle et al. (1998) suggest that some of the low-luminosity broad-line radio galaxies are true quasars which are not sufficiently bright to be classified as such in the optical. If so, then reassigning them to the HEGs rather than to the quasars will decrease the fraction of quasars, resulting in small opening angles and the consequence of this is that  $\bar{\theta}_{cf} = 24^\circ$  is underestimated in the  $L_{[O III]}$  low-luminosity bin (Table 2). In a  $L_{[O III]}$  high-luminosity bin the fraction of quasars may increase if the [O III] emitting region is partially obscured in radio galaxies causing a factor of 5 to 10 depression of the [O III] emission (Hes et al. 1996) which may result in the overestimation of  $\bar{\theta}_{cf}$ . The selection effects at low- and high-luminosities may reproduce a positive correlation between  $\bar{\theta}_{cf}$  and  $L_{[O III]}$ . To understand the bias introduced in the fraction of quasars one may consider the independent measurements of the opening angle  $\bar{\theta}_{cs}$  (Table 2). The fact that  $\bar{\theta}_{cs}$  is independent of the fraction of quasars (eq. 7),  $\bar{\theta}_{cs}$  positively correlates with  $L_{[O III]}$  (Fig. 4) and  $\bar{\theta}_{cs} \approx \bar{\theta}_{cf}$  across  $L_{[O III]}$  range indicates that the  $\bar{\theta}_{cf} - L_{[O III]}$  correlation is real and if there is a bias in the fraction of quasars it is not significant. The  $\chi^2$  test is used to estimate the significance of the null hypothesis that two independent measurements of  $\bar{\theta}_{cs}$  and  $\bar{\theta}_{cf}$  are equal across the  $L_{[O III]}$

and  $L_{151}$  ranges. For two and three sets of binned data the values of  $\bar{\theta}_{cs}$  and  $\bar{\theta}_{cf}$  are not significantly different ( $P < 80\%$ ). Figs. 4 and 5 show that  $\bar{\theta}_{cs} \approx \bar{\theta}_{cf}$  in different bins of  $L_{[O III]}$  and  $L_{151}$ . The equality of two independent estimates confirms the validity of the orientation-based unification scheme for radio galaxies and quasars and it indicates that the relative mean size of quasars ( $\bar{l}_Q/\bar{l}$ ) and the relative number of quasars ( $N_Q/N_{G+Q}$ ) are indeed good measures of the critical viewing angle in the low-frequency radio samples.

Another possible selection effect is related to the measured projected sizes of FR II sources which may be overestimated as a result of projection of the volume of radio lobes. It is clear that independent of the plausible geometry of radio lobes the projection effects may be important for sources having small inclinations of radio axes to the line of sight. The fact that the exclusion of small sizes ( $< 20$  kpc, see section 3) does not change the final results indicates that the projection effect is not likely to influence strongly the estimates of  $\theta_{cs}$ .

The assumption that the axis of a dusty torus is aligned with the radio axis of FR II sources can be partially relaxed (e.g., Capetti & Celotti 1999) in real life allowing some distribution of angles between the axes of the torus and the jet. In this scenario there should be a difference between the true critical angle ( $\theta_{ct}$ ) defined by the geometry of the torus and the critical angle  $\theta_{cs}$  (eq. 7) estimated by means of projected sizes of FR II sources. It is important to understand how this difference varies depending on the value of true critical angle and whether it can lead to a positive correlation found between  $\theta_{cs}$  and  $L_{[O III]}$ . To test this, I model random angles between the axes of the torus and the jet by generating a pair of 5000 random directions: for every random axis of the torus the random jet direction is generated within the specified cone angle  $2\delta_{max}$ . For simplicity, a single linear size (300 kpc) for radio galaxies and quasars is adopted. Then, given the true critical angle ( $\theta_{ct}$ ), I generate the projected linear sizes for both quasars and all sources using the inclination angles of the jet. The mean sizes of quasars and the whole sources are used to estimate the critical angle  $\theta_{cs}$  (eq. 7). The deviation of estimated critical angle  $\theta_{cs}$  from the true  $\theta_{ct}$  one is presented in Table 4 for different  $\delta_{max}$ .  $\delta_{max} = 0$  corresponds to the case where the axes are aligned and here there is an excellent agreement between  $\theta_{ct}$  and  $\theta_{cs}$ , which provides a good test of the formalism involved in equation (7). For larger values of  $\delta_{max}$  the estimated critical angle appears to be larger than the true critical angle ( $\theta_{cs} > \theta_{ct}$ ) (Table 4). One may conclude that the effect of misalignment of axes of the torus and the jet leads to the overestimation of critical angles  $\theta_{cs}$ , which is higher for small  $\theta_{ct}$ . If there is a significant misalignment of axes then the critical angles in the  $\theta_{cs} - L_{[O III]}$  relation plane are overestimated with the effect of making flatter the slope of the real  $\theta_{ct} - L_{[O III]}$  relation. This demonstrates that the misalignment effect makes the real correlation weaker and thus can not produce the positive correlation found between  $\theta_{cs}$  and  $L_{[O III]}$ .

## 5. Discussion and conclusions

The key result of the previous section is that the opening angle of the ionizing cone of the torus becomes larger at high [O III] emission-line luminosities. The half opening angle  $\tan \theta_c =$

**Table 4.** The values of true critical angles  $\theta_{\text{ct}}$  and their deviations ( $\theta_{\text{cs}}$ ) simulated for different half cone angles  $\delta_{\text{max}}$  within which the angles between the axes of the torus and the jet are distributed.

$\theta_{\text{ct}}^\circ$	$\theta_{\text{cs}}^\circ \pm \sigma_{\theta_{\text{cs}}}$			
	$\delta_{\text{max}} = 0^\circ$ ( $\theta_{\text{ct}} = \theta_{\text{cs}}$ )	$\delta_{\text{max}} = 10^\circ$	$\delta_{\text{max}} = 20^\circ$	$\delta_{\text{max}} = 30^\circ$
20	$19.8 \pm 0.4$	$21.6 \pm 0.5$	$26.5 \pm 0.7$	$34.9 \pm 0.9$
40	$39.5 \pm 0.5$	$40.2 \pm 0.5$	$42.8 \pm 0.6$	$47.0 \pm 0.7$
60	$59.3 \pm 0.6$	$59.9 \pm 0.3$	$61.2 \pm 0.7$	$63.4 \pm 0.7$

$2r/h$  depends on the inner radius,  $r$ , of the torus and its height,  $h$  (the thickness of the dusty torus). In extreme cases, the positive correlation between  $\theta_{\text{c}}$  and  $L_{[\text{O III}]}$  can be interpreted as (i) a systematic increase of the radius of the torus with  $L_{[\text{O III}]}$ , or (ii) decrease of the height with  $L_{[\text{O III}]}$ . The first relation naturally follows from the receding torus model (Lawrence 1991; Hill et al. 1996). In this model (i) the ionizing radiation from the AGN evaporates the circumnuclear dust forming the inner wall of the torus at a distance  $r$  which increases as  $r \sim L_{[\text{O III}]}^{0.5}$  (where  $L_{[\text{O III}]}$  is assumed to be a measure of the ionizing luminosity), and (ii) the height of the torus  $h$  is independent of  $L_{[\text{O III}]}$ . There is observational evidence in favour of an  $r$ - $L_{[\text{O III}]}$  relation. Minezaki et. al. (2004) used multi-epoch observations of the Seyfert 1 galaxy NGC 4151 to show that the time lag between the optical and near-infrared light curves grows with optical luminosity as  $\log \Delta t \propto L^{0.5}$ . They interpreted this as thermal dust reverberation in an AGN to relate a  $\Delta t$  to the inner radius of the dusty torus ( $\Delta t \propto r$ ). Willott et al. (2002) found that 3C/6C quasars have higher submillimetre luminosities by a factor  $> 2$  than radio galaxies. They argued that this is in quantitative agreement with the receding torus model if there is a positive correlation between optical and far-infrared luminosities. Another piece of evidence comes from the studies of the mid-infrared spectra of 3C radio sources (Freudling et al. 2003). They showed that the bands of polycyclic aromatic hydrocarbons (PAHs) are weak in broad-line radio galaxies and they are much stronger in narrow-line radio galaxies of similar luminosities. They interpreted this difference as a result of the heating radiation from the central nucleus: the hard radiation destroys PAHs in the broad-line regions and heats larger dust grains at intermediate distances. The spectra of broad-line galaxies and quasars originate in the broad-line region where only few PAHs survive. In the narrow-line radio galaxies this region is obscured and the spectra are dominated by cooler dust at larger distances where more PAHs can survive. Simpson & Rawlings (2000) showed that the near-infrared spectral slopes of 3CR quasars are steeper for less luminous objects and that the fraction of moderately obscured, red quasars decreases with increasing radio luminosity. Both relations are in agreement with the receding torus model.

As indicated by Simpson (2003) there are several lines of evidence indicating that the height of the torus is not a strong function of luminosity. If so, the half opening angle of the torus  $\tan \theta_{\text{c}} = 2r/h \propto L_{[\text{O III}]}^{0.5}/h$  should increase with  $[\text{O III}]$  emission line luminosity even if there is a spread in  $h$ . This trend is in agreement with the positive correlation found between the half

opening angle of the torus and  $[\text{O III}]$  emission-line luminosity (Fig. 4). To fit the  $\theta_{\text{c}} - L_{[\text{O III}]}$  positive correlation, I used the relation predicted by the receding torus model,  $\tan \theta_{\text{c}} \propto L_{[\text{O III}]}^A$ , where  $A$  is a free parameter. Using the measurements of  $\bar{\theta}_{\text{cs}}$  and  $\bar{\theta}_{\text{ct}}$ , and  $\bar{L}_{[\text{O III}]}$  (see Table 2) I calculate the power-law indices  $A_s = 0.35 \pm 0.08$  and  $A_f = 0.26 \pm 0.02$  corresponding to  $\bar{\theta}_{\text{cs}}$  and  $\bar{\theta}_{\text{ct}}$  respectively. The value 0.35 is in agreement with the predicted value of 0.5 ( $r \propto L_{[\text{O III}]}^{0.5}$ ) within  $\sim 2\sigma$  significance level. It is likely that the use of the averaged critical angles and small number of points result in a smoothing of the real relation, which results in smaller values of  $A_s$  and  $A_f$  compared with the predicted one, 0.5. Larger values of  $A_s = 0.44$  and  $A_f = 0.27$  are found when the number of  $L_{[\text{O III}]}$  bins are doubled. The range of  $A \sim (0.3 \text{ to } 0.4)$  is a plausible estimate for both  $A_s$  and  $A_f$ . If these values are correct then in order to fit the receding torus model one should expect that the height of the torus also correlates positively with the emission-line luminosity in the form  $h \propto L_{[\text{O III}]}^B$  where  $B \sim (0.1 \text{ to } 0.2)$ . From the consideration of the ratio of the near-infrared luminosity to the bolometric luminosity for Palomar-Green quasars, Cao (2005) found significant correlation between the torus thickness and the bolometric luminosity,  $h \propto L_{\text{bol}}^{0.37 \pm 0.05}$ , which is somewhat stronger than is expected from my results. A larger sample of radio sources is needed to confirm the increase of the torus thickness with photoionizing radiation of the AGN.

The second relation, i.e. the negative correlation between  $h$  and  $L_{[\text{O III}]}$  which may be a cause for an increase of  $\bar{\theta}_{\text{c}}$  with  $L_{[\text{O III}]}$ , seems to be unrealistic since it requires the inner radius of the torus to be independent of  $L_{[\text{O III}]}$ . One may conclude that the growth of the opening angle of the torus with increasing  $L_{[\text{O III}]}$  is a direct evidence of the receding-torus-like structures around central nuclei of FR II radio sources. This result apparently breaks the degeneracy (multi-population or receding torus) in the interpretation of data in favor of the receding torus model.

The main conclusions of this analysis are as follows:

1. On the basis of an inverse problem approach, an equation for estimating the opening angle of the torus by means of the mean projected linear sizes of FR II radio galaxies and quasars has been derived. The small errors involved in estimation of the opening angle makes the linear size statistics a powerful tool for investigating the orientation-dependent structures in AGN.

2. An application of this equation to the combined complete sample of FRII radio sources revealed the following:
  - The mean half opening angle of the torus is  $42^\circ \pm 7^\circ$  for the whole sample.
  - Statistically significant positive correlation is found between the opening angle of the torus and [O III] emission-line luminosity. The mean half opening angle grows from  $\sim 20^\circ$  to  $\sim 60^\circ$  between  $L_{[\text{O III}]} \sim 10^{35}$  W to  $10^{37}$  W. This dependence favours the receding torus model and is fitted with the  $\tan \theta_c \propto L_{[\text{O III}]}^{0.35}$  relation.
  - No significant changes of the opening angle are found either with radio luminosity or cosmic epoch.
  - Two independent measurements of the half opening angle are correlated across [O III] emission-line and radio luminosity ranges. This supports the validity of the unified scheme of AGN and obscuring torus model. It also confirms that the mean relative size and relative number of quasars in low-frequency radio samples can serve as good estimators of the opening angle of an obscuring material.

*Acknowledgements.* I am very grateful to Chris Simpson and Martin Hardcastle for many valuable comments, to Moshe Elitzur and Thomas Beckert for useful discussions and comments, to Steve Rawlings for kindly supplying the electronic version of the 6CE/7CR databases and for discussions, and to Alan Roy for useful comments and critical reading of a draft of the paper. I also thank the anonymous referee for careful reading of the manuscript and valuable suggestions, and I thank the Alexander von Humboldt Foundation for the award of a Humboldt fellowship.

## References

- Allen, S. W., & Fabian, A. C. 1992, MNRAS, 258, 29  
 Antonucci, R. R. J., & Miller, J. S. 1985, ApJ, 297, 621  
 Arshakian, T. G., & Longair, M. S. 2000, MNRAS, 311, 846  
 Barthel, P. D. 1989, ApJ 336, 606  
 Bondi, M., Brunetti, G., Comastri, A., & Setti, G. 2004, MNRAS, 354, L43  
 Brunetti, G., Setti, G., & Comastri, A. 1997, A&A, 325, 898.  
 Brunetti, G., Cappi, M., Setti, G., Feretti, L., & Harris, D. E. 2001, A&A, 372, 755  
 Canalizo, G., Max, C., Whysong, D., Antonucci, R., & Dahm, S.E. 2003, ApJ, 597, 823  
 Cao, X. 2005, ApJ, 619, 86  
 Capetti, A., & Celotti, A. 1999, MNRAS, 304, 434  
 Chandrasekhar, S., & Munch, G. 1950, ApJ, 111, 142  
 Fanaroff, B. L., & Riley, J. M. 1974, MNRAS, 167, 31P  
 Freudling, W., Siebenmorgen, R., & Haas, M. 2003, ApJ, 599, L13  
 Garrington, S. T., Leahy, J. P., Conway, R. G., & Laing, R. A. 1988, Nature, 331, 147  
 Gopal-Krishna, Kulkarni, V. K., & Wiita, P. J. 1996, ApJ, 463, L1  
 Grimes, J. A., Rawlings, S., & Willott, C. J. 2004, MNRAS, 349, 503  
 Haas, M., Müller, S. A. H., Bertoldi, F., et al. 2004, A&A, 424, 531  
 Hardcastle, M. J., Alexander, P., Pooley, G. G., & Riley, J. M. 1998, MNRAS, 296, 445  
 Hes, R., Barthel, P.D., & Fosbury, R.A.E. 1996, A&A, 313, 423  
 Hill, G. J., Goodrich, R. W., & DePoy, D. L. 1996, ApJ, 462, 163  
 Jaffe, W., Ford, H. C., Ferrarese, L., van den Bosch, F., & O'Connell, R.W. 1993, Nature, 364, 213

- Laing, R. A., Jenkins, C. R., Wall J. C., & Unger, S. W. 1994, in Bicknell G. V., Dopita M. A., Quinn P. J., eds, The First Stromolo Symposium: The Physics of Active Galaxies, ASP Conf. Ser. 54, San Francisco, 201  
 Laing, R. A., Riley, J.M., & Longair, M. S. 1983, MNRAS, 204, 151  
 Laing, R. A. 1988, Nature, 331, 149  
 Lawrence, A. 1991, MNRAS, 252, 586  
 McLure, R. J., & Dunlop, J. S. 2002, MNRAS, 331, 795  
 Meisenheimer, K., Haas, M., Müller, S. A. H., Chini, R., Klaas, U., & Lemke, D. 2001, A&A, 372, 719  
 Miller, J. S., & Goodrich, R. W. 1990, ApJ, 355, 456  
 Minezaki, T., Yoshii, Y., Kobayashi, Y., Enya K., Suganuma, M., Tomita, H., Aoki, T., & Peterson, B. A. 2004, ApJ, 600, L35  
 Rawlings, S., Eales, S., & Lacy, M. 2001, MNRAS, 322, 523  
 Saikia, D. J., & Kulkarni, V. K. 1994, MNRAS, 270, 897  
 Scheuer, P. A. G. 1987, in Zensus J., Pearson T., eds, Superluminal Radio Sources, Cambridge University Press, Cambridge, 104  
 Siebenmorgen, R., Freudling, W., Krügel, E., & Haas, M. 2004, A&A, 42, 129  
 Simpson, C., Rawlings, S., & Lacy, M. 1999, MNRAS, 306, 828  
 Simpson, C., & Rawlings, S. 2000, MNRAS, 317, 1023  
 Simpson, C. 2003, in High-redshift Radio Galaxies - Past, Present and Future, eds M. J. Jarvis & H. J. A. Röttgering, New Astronomy Reviews, 211  
 Ueno, S., Koyama, K., Nishida, M., Yamauchi, S., & Ward, M. J. 1994, ApJ, 431, L1  
 Verdoes Kleijn, G. A., de Zeeuw, P. T., Baum, S. A., O'Dea, C. P., van der Marel, R. P., Xu, C., Carollo, C. M., & Noel-Storr, J. 2001, in IAU Symp. 206, Galaxies and Their Constituents at the Highest Angular Resolutions, ed. R. T. Schilizzi (San Francisco: ASP), 62  
 Vermeulen, R. C., & Cohen, M. H. 1994, ApJ, 430, 467  
 Willott, C. J., Rawlings, S., Blundell, K. M., & Lacy M. 2000, MNRAS, 316, 449  
 Willott, C. J., Rawlings, S., Archibald, E. N., & Dunlop, J. S. 2002, MNRAS, 331, 435

## APPENDIX: Equation for estimating the critical viewing angle

Suppose, we have a population of double radio sources with radio axes oriented randomly in space. The objects are classified as radio galaxies if the viewing angle between the axis of the obscuring 'torus' and the line of the sight is larger than a critical angle defined by a half opening angle of the torus,  $\theta > \theta_c$ , otherwise, if  $\theta < \theta_c$ , they are viewed as radio quasars. There is observational evidence that the axis of a radio jet is aligned with the axis of the torus (Jaffe et al. 1993; Verdoes Kleijn et al. 2001; Canalizo et al. 2003). Assume that radio axes of FRII radio sources are aligned with the axes of obscuring tori. Then the half opening angle of the torus is measured by the angle ( $\theta_{cs}$ ) between the radio axis and the critical angle  $\theta_c$ , i.e.  $\theta_c \approx \theta_{cs}$ . The task is to derive an equation which allows  $\theta_{cs}$  to be estimated given the distribution function of projected linear sizes of radio galaxies and quasars,  $f(l)$ .

The projected linear size  $l = l_0 \sin \theta$ , where  $l_0 \in [0, l_m]$  is the deprojected linear size ( $l_m$  being the largest linear size in the sample), and  $\theta \in [0, \pi/2]$  is the angle between the radio axis (or axis of the torus) and the line of sight. Assume that torus axes are distributed isotropically over the sky,  $K(\theta) = \sin \theta$ , then,

$$f(l) = l \int_l^{l_m} \frac{F(l_0) dl_0}{l_0 \sqrt{l_0^2 - l^2}}, \quad (2)$$

where  $F(l_0)$  is the distribution function of linear sizes. This integral equation was first derived by Chandrasekhar & Munch (1950) for the problem of reconstruction of the distribution of stellar rotation velocities.

The mean linear size of the whole sample is given by,

$$\bar{l}_0 = \frac{4}{\pi} \bar{l}. \quad (3)$$

For quasars ( $\theta < \theta_{cs}$ ) the equation (2) can be written as,

$$f(l) = C_Q l \int_{l/\sin\theta_{cs}}^{l_m} \frac{F(l_0) dl_0}{l_0 \sqrt{l_0^2 - l^2}} \quad (l \leq l_m \sin\theta_{cs}), \quad (4)$$

where  $C_Q = 1/(1 - \cos\theta_{cs})$ . The equation for the moments is,

$$\nu_n = C_Q \nu_{0n} \int_0^{l_m \sin\theta_{cs}} \frac{l^{n+1} dl}{l_0^{n+1} \sqrt{l_0^2 - l^2}}, \quad (5)$$

and the first moment, which corresponds to the mean linear size of quasars,

$$(\bar{l}_0)_Q = 2\bar{l}_Q \frac{1 - \cos\theta_{cs}}{\theta_{cs} - \sin\theta_{cs} \cos\theta_{cs}}. \quad (6)$$

The radio galaxies and quasars have the same distribution of linear sizes, hence  $(\bar{l}_0)_Q = \bar{l}_0$ . From (3) and (6) one may recover the equation for estimating the critical viewing angle,

$$\frac{\pi \bar{l}_Q}{2 \bar{l}} = \frac{\theta_{cs} - \sin\theta_{cs} \cos\theta_{cs}}{1 - \cos\theta_{cs}}. \quad (7)$$

Given the standard errors of the mean projected linear sizes of quasars  $\sigma_{\bar{l}_Q}$  and the whole population  $\sigma_{\bar{l}}$ , one can estimate the standard error of the critical angle,

$$\sigma_{\theta_{cs}}^2 = \left( \frac{\partial \theta_{cs}}{\partial \bar{l}} \right)^2 \sigma_{\bar{l}}^2 + \left( \frac{\partial \theta_{cs}}{\partial \bar{l}_Q} \right)^2 \sigma_{\bar{l}_Q}^2, \quad (8)$$

where,

$$\frac{\partial \theta_{cs}}{\partial \bar{l}} = \frac{2(\theta_{cs} - \sin\theta_{cs} \cos\theta_{cs})^2}{\pi A \bar{l}_Q}, \quad (9)$$

$$\frac{\partial \theta_{cs}}{\partial \bar{l}_Q} = -\frac{\pi(1 - \cos\theta_{cs})^2}{2 A \bar{l}}, \quad (10)$$

$$A = \sin\theta_{cs}(\theta_{cs} - \sin\theta_{cs} \cos\theta_{cs}) - 2\sin^2\theta_{cs}(1 - \cos\theta_{cs}). \quad (11)$$

If there is a spread in  $\theta_{cs}$  then eqs. (7-11) can be used for estimating the mean half opening angle of the torus  $\bar{\theta}_{cs}$  and its standard error  $\sigma_{\bar{\theta}_{cs}}$ .

Let us investigate the errors associated with critical angles ( $\theta_{cs}$  and  $\theta_{cf}$ ) defined by the mean size and fraction of quasars respectively (eqs. 7 and 1). For this, I adopt the mean linear size of  $N_{G+Q} = 206$  radio galaxies and quasars,  $\bar{l} = (279 \pm 21)$  kpc (see section 4), and the mean size of  $N_Q = 52$  quasars,  $\bar{l}_Q = (162 \pm 19)$  kpc, from the combined sample of FR II radio sources (see section 3). I assume that the ratios  $\sigma_{\bar{l}}/\bar{l} = 0.075$  and  $\sigma_{\bar{l}_Q}/\bar{l}_Q = 0.099$  are constant for any critical angle  $\theta_{cs}$ .

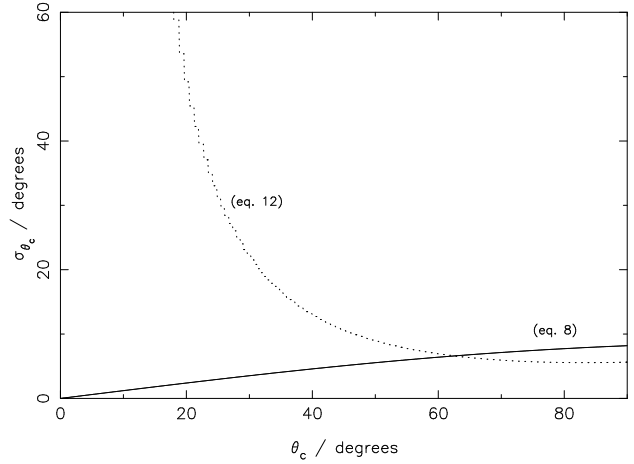


**Fig. 6.** Functional relation between the half opening angle of the torus and its standard error is presented for equation (8) (solid line) and equation (12) (dotted line).

For any given  $\theta_{cs}$ , I calculate  $\sigma_{\theta_{cs}}$  from eqs. (8-11) using the estimates of  $\bar{l}_Q$  (eq. 7) and its standard error (provided that their inverse ratio is equal to 0.099). The  $\sigma_{\theta_{cs}} - \theta_{cs}$  dependence is shown in Fig. 6 (solid line). The relation between  $\sigma_{\theta_{cf}}$  and  $\theta_{cf}$  (dashed line) is drawn on the assumptions that (i)  $\sigma_{N_{G+Q}} = \sqrt{N_{G+Q}} \approx 14$  and  $\sigma_{N_Q} = \sqrt{N_Q} \approx 7$ , and that (ii) the ratios  $\sigma_{N_{G+Q}}/N_{G+Q} = 0.068$  and  $\sigma_{N_Q}/N_Q = 0.13$  are unchanged over  $\theta_{cf}$ . Given the  $\theta_{cf}$ , one may calculate,

$$\sigma_{\theta_{cf}}^2 = \left( \frac{\partial \theta_{cf}}{\partial N_{G+Q}} \right)^2 \sigma_{N_{G+Q}}^2 + \left( \frac{\partial \theta_{cf}}{\partial N_Q} \right)^2 \sigma_{N_Q}^2, \quad (12)$$

where,

$$\frac{\partial \theta_{cf}}{\partial N_{G+Q}} = -\frac{N_Q}{N_{G+Q}^2} \left( 1 - \left( 1 - \frac{N_Q}{N_{G+Q}} \right)^2 \right)^{-1/2}, \quad (13)$$

$$\frac{\partial \theta_{cf}}{\partial N_Q} = \frac{1}{N_{G+Q}} \left( 1 - \left( 1 - \frac{N_Q}{N_{G+Q}} \right)^2 \right)^{-1/2}. \quad (14)$$

One can see (Fig. 6) that the errors,  $\sigma_{\theta_{cf}}$  and  $\sigma_{\theta_{cs}}$ , are comparable at angles  $> 50^\circ$ . At smaller angles, the  $\sigma_{\theta_{cf}}$  grows exponentially, reaching the value of  $50^\circ$  at  $\theta_c = 20^\circ$ , whilst  $\sigma_{\theta_{cs}}$  decreases gradually to zero degrees. The important implication of this analysis is that the errors associated with  $\theta_{cs}$  are small indicating that the linear size statistics is a powerful tool for studying the correlations between the opening angle of the torus and physical characteristics of AGN in the low-frequency radio samples. This approach also can be used to estimate the opening angle of structures (around the central engines of double radio sources) showing the orientation-dependent physical/spectral characteristics.